



# Design Requirements for Group-IV Laser Based on Fully Strained $\text{Ge}_{1-x}\text{Sn}_x$ Embedded in Partially Relaxed $\text{Si}_{1-y-z}\text{Ge}_y\text{Sn}_z$ Buffer Layers

Yosuke Shimura,<sup>a,b,e,z</sup> Srinivasan Ashwyn Srinivasan,<sup>a,c,d</sup> and Roger Loo<sup>a,\*</sup>

<sup>a</sup>imec, Leuven 3001, Belgium

<sup>b</sup>Department of Physics, KU Leuven, Leuven, Belgium

<sup>c</sup>Photonics Research Group (INTEC), Ghent University-IMEC, Ghent, Belgium

<sup>d</sup>Center for Nano- and Biophotonics (NB-Photonics), Ghent University, Ghent, Belgium

Theoretical calculation using the model solid theory is performed to design the stack of a group-IV laser based on a fully strained  $\text{Ge}_{1-x}\text{Sn}_x$  active layer grown on a strain relaxed  $\text{Si}_{1-y-z}\text{Ge}_y\text{Sn}_z$  buffer/barrier layer. The degree of strain relaxation is taken into account for the calculation for the first time. The transition between the indirect and the direct band material for the active  $\text{Ge}_{1-x}\text{Sn}_x$  layer is calculated as function of Sn content and strain. The required Sn content in the buffer layer needed to apply the required strain in the active layer in order to obtain a direct bandgap material is calculated. Besides, the band offset between the (partly) strain relaxed  $\text{Si}_{1-y-z}\text{Ge}_y\text{Sn}_z$  buffer layer and the  $\text{Ge}_{1-x}\text{Sn}_x$  pseudomorphically grown on it is calculated. We conclude that an 80% relaxed buffer layer needs to contain 13.8% Si and 14% Sn in order to provide sufficiently high band offsets with respect to the active  $\text{Ge}_{1-x}\text{Sn}_x$  layer which contains at least 6% Sn in order to obtain a direct bandgap.

© The Author(s) 2016. Published by ECS. This is an open access article distributed under the terms of the Creative Commons Attribution 4.0 License (CC BY, <http://creativecommons.org/licenses/by/4.0/>), which permits unrestricted reuse of the work in any medium, provided the original work is properly cited. [DOI: 10.1149/2.0301605jss] All rights reserved.

Manuscript submitted December 21, 2015; revised manuscript received March 7, 2016. Published March 17, 2016. This was Paper 1826 presented at the Cancun, Mexico, Meeting of the Society, October 5–9, 2014.

The ever-increasing need for high speed communication between chips have resulted in a long term search for an alternative solution, namely optical interconnects, aiming a replacement of conventional electrical interconnects that suffer from high-power consumption.<sup>1,2</sup> Among the basic building blocks, like waveguides, photodetectors, modulators and filters, needed for an optical link, the on-chip laser source is another key component. For on-chip laser source applications, Ge is a promising material as it can be easily grown on a Si platform as compared to III-V materials. Since Ge is intrinsically an indirect bandgap material, the light emitting properties of such a material are very poor. However, due to the relatively small difference between the indirect (0.66 eV) and direct bandgap (0.8 eV), the semiconductor community has looked into a number of methods to transform the indirect band-gap material to a direct band-gap material.<sup>3–5</sup>

One method to obtain a direct bandgap group IV material is by applying tensile strain to Ge, which changes its band structure, as previously proposed by Fischetti et al.<sup>5</sup> If biaxial tensile strain is applied, the direct bandgap shrinks faster than the indirect bandgap. Fischetti et al. calculated the required biaxial tensile strain to be 1.4% to obtain a direct bandgap.<sup>5</sup> The second option is by adding a sufficiently large amount of Sn to the Ge matrix forming a  $\text{Ge}_{1-x}\text{Sn}_x$  alloy.<sup>4,6,7</sup> As the introduction of strain and Sn both modify the band structure of Ge, theoretical analysis is required to quantify the critical Sn content to obtain a direct bandgap material for different strain conditions.

In order to apply strain to the active  $\text{Ge}_{1-x}\text{Sn}_x$  layer, a buffer layer with a specific lattice constant could be used. The buffer layer needs to be strain relaxed to achieve its bulk lattice constant because it is generally grown on a Si platform. This strain relaxed buffer (SRB) layer does not only require a controlled lattice constant but also a large bandgap to enable effective carrier confinement in the active  $\text{Ge}_{1-x}\text{Sn}_x$  layer in both the conduction and valence bands. As a result,  $\text{Si}_{1-y-z}\text{Ge}_y\text{Sn}_z$  is a potentially suitable material for the buffer and barrier layers because the lattice constant and the energy bandgap can be simultaneously controlled by choosing appropriate Sn and Si contents.<sup>8,9</sup> Therefore, we propose to use an epitaxial stack layer consisting of a direct bandgap  $\text{Ge}_{1-x}\text{Sn}_x$  active layer coherently grown on a  $\text{Si}_{1-y-z}\text{Ge}_y\text{Sn}_z$  SRB for a group IV laser with a high optical gain. A

similar proposal has been made by Chang et al.<sup>10</sup> However, in practice it is difficult to obtain fully relaxed  $(\text{Si}_{1-y-z})\text{Ge}_y\text{Sn}_z$ .<sup>11–13</sup> Therefore, the degree of strain relaxation (DSR) needs also to be considered when designing the material stack of the target laser devices. The low solubility limit of Sn into Ge and Si restricts us to use an as low as possible Sn content.<sup>14</sup> As a result, this manuscript aims to propose a material stack for laser devices consisting of group IV elements with the lowest possible but sufficient Sn content to obtain direct bandgap characteristics.

Using the model solid theory approach, we will first calculate the required Sn content in  $\text{Ge}_{1-x}\text{Sn}_x$  as a function of strain to obtain a direct bandgap material.<sup>15</sup> The parameters we used have been taken from literatures. Some of these theoretical values have also been confirmed experimentally. We then estimate the bandgap of the  $\text{Si}_{1-y-z}\text{Ge}_y\text{Sn}_z$  SRB layer using the same theory to extract the conduction and valence band offsets with respect to the pseudomorphically strained  $\text{Ge}_{1-x}\text{Sn}_x$  active region. The DSR is varied in our modelling. Finally, we will propose a layer stack for an electrically pumped laser device taking the shift of the Fermi level position caused by impurity doping into account.

## Modeling Framework

We first calculate the bandgap energies for strain free  $(\text{Si}_{1-y-z})\text{Ge}_y\text{Sn}_z$  layers using Vegard's law taking bowing effects into account. Next, we discuss the strain induced energy shift as calculated by using the model solid theory.<sup>15</sup>

In  $(\text{Si}_{1-y-z})\text{Ge}_y\text{Sn}_z$ , hydrostatic stress linearly shifts the energy positions of the L-point,  $E_{cL}$  and the  $\Gamma$ -point,  $E_{c\Gamma}$ , in the conduction band and  $E_{v,av}$ , the average energy of the uppermost 3 valence bands (light hole, heavy hole and spin-orbit split-off band) at the  $\Gamma$  point of the band-structure. The energy shifts can be expressed as:

$$\Delta E_{ci} = a_{ci}(\epsilon_{xx} + \epsilon_{yy} + \epsilon_{zz}) \quad [1a]$$

$$\Delta E_{v,av} = a_v(\epsilon_{xx} + \epsilon_{yy} + \epsilon_{zz}) \quad [1b]$$

where  $\Delta E_c$  and  $\Delta E_{v,av}$  denote the energy shift by strain for the conduction band and the average valence band, respectively. For the conduction band, the energy shift at different k-space of the energy band diagram ( $i = \Gamma$  or L) are considered to determine whether the bandgap is direct or indirect.  $a_{ci}$  and  $a_v$  represent the hydrostatic deformation

\*Electrochemical Society Member.

<sup>z</sup>Present address: Graduate School of Engineering, Nagoya University, Nagoya, Japan.

<sup>e</sup>E-mail: yshimura@alice.xtal.nagoya-u.ac.jp

**Table I.** Material parameters used for the calculation (at room temperature). Values are from Ref. 10 except those with indications.

|                                      |                         | Si                     | Ge                       | Sn                    |
|--------------------------------------|-------------------------|------------------------|--------------------------|-----------------------|
| Lattice constant                     | a (nm)                  | 0.54307                | 0.56573                  | 0.64892               |
| Average valence band energies        | $\Delta E_{v,ave}$ (eV) | -0.75 <sup>10,17</sup> | 0                        | 0.85 <sup>10,17</sup> |
| Band gaps                            | $E_{g,\Gamma}$ (eV)     | 4.185                  | 0.7985                   | -0.413                |
|                                      | $E_{g,L}$ (eV)          | 1.65                   | 0.664                    | 0.092                 |
|                                      | $\Delta_{so}$ (eV)      | 0.044                  | 0.29                     | 0.8                   |
|                                      | $a_{c,\Gamma}$ (eV)     | -9.64 <sup>18</sup>    | -7.50 <sup>18</sup>      | -5.75 <sup>18</sup>   |
| Deformation potentials               | $a_{c,L}$ (eV)          | -1.42 <sup>19</sup>    | -1.46 <sup>20</sup>      | -2.14 <sup>21</sup>   |
|                                      | $a_v$ (eV)              | 2.28 <sup>18</sup>     | 2.14 <sup>18</sup>       | 1.51 <sup>18</sup>    |
|                                      | $b_s$ (eV)              | -2.1                   | -1.88 <sup>22</sup>      | -2.7                  |
|                                      | $C_{11}$ (GPa)          | 165.77                 | 128.53                   | 69                    |
| Elastic constants                    | $C_{12}$ (GPa)          | 63.93                  | 48.26                    | 29.3                  |
|                                      |                         |                        |                          |                       |
| Bowing parameters for $Ge_{1-x}Sn_x$ | $b_L$ (eV)              |                        | 1.11-0.78x <sup>23</sup> |                       |
|                                      | $b_\Gamma$ (eV)         |                        | 2.66-5.4x <sup>23</sup>  |                       |
|                                      | $b_l$ (nm)              |                        | 0.0041 <sup>12</sup>     |                       |
| Bowing parameters for $Si_{1-y}Ge_y$ | $b_L$ (eV)              |                        | 0.169                    |                       |
|                                      | $b_\Gamma$ (eV)         |                        | 0.21                     |                       |
|                                      | $b_l$ (nm)              |                        | -0.0026 <sup>16</sup>    |                       |

potential for the conduction band at the  $\Gamma$  or L valley and the valence band, respectively.  $\varepsilon_{xx}$  and  $\varepsilon_{yy}$  denote the strain in the  $(Si_{1-y-z})Ge_ySn_z$  layer in the direction parallel to the  $(Si_{1-y-z})Ge_ySn_z$ /substrate interface, and  $\varepsilon_{zz}$  is the strain perpendicular to the plane of the interface. The impact of DSR is considered in these strain values. In order to estimate the strain, the lattice constant of  $(Si_{1-y-z})Ge_ySn_z$  was estimated using Vegard's law with bowing parameters of for lattice constant,  $b_l$ .<sup>12,16</sup> We assume the bowing parameter for the  $Si_{1-z}Sn_z$  lattice constant to be 0.

In addition, the shear components of the strain lead to additional splitting in the valence bands, their relative positions from  $E_{v,av}$  can be expressed as:<sup>15</sup>

$$\Delta E_{v,hh} = \frac{1}{3}\Delta_0 - \frac{1}{2}\delta E_{001} \quad [2a]$$

$$\Delta E_{v,lh} = -\frac{1}{6}\Delta_0 + \frac{1}{4}\delta E_{001} + \frac{1}{2}\left[\Delta_0^2 + \Delta_0\delta E_{001} + \frac{9}{4}(\delta E_{001})^2\right]^{1/2} \quad [2b]$$

where  $\Delta E_{v,hh}$  and  $\Delta E_{v,lh}$  are the energy shifts for the heavy and light hole bands, respectively.  $\Delta_0$  denotes spin-orbit splitting, and  $\delta E_{001} = 2b_s(\varepsilon_{zz} - \varepsilon_{xx})$ , where  $b_s$  is the shear deformation potential. For the conduction band at the L point, we do not have to consider this additional splitting by shear components of the strain as the 8 valleys along  $\langle 111 \rangle$  can be treated as equivalent when stressed along the  $(001)$  plane for a  $(Si_{1-y-z})Ge_ySn_z$  material. As a result, the bandgap of strained  $(Si_{1-y-z})Ge_ySn_z$  can be calculated from the bandgap of an relaxed layer together with the energy shift caused by strain.

All other parameters, represented as  $P_{SiGeSn}$ , except the bandgap and lattice constant were linearly interpolated as:

$$P_{SiGeSn} = P_{Si}(1-y-z) + P_{Ge}y + P_{Sn}z \quad [3]$$

A summary of the material parameters used in this work for pure Si, Ge and Sn is listed in Table I. The impact of strain on these parameters has not been reported in literature and therefore, these strain effects are not considered in Eq. 3.

## Results

**Transition to direct bandgap material for  $Ge_{1-x}Sn_x$ .**—The calculated lowest bandgap energy of  $Ge_{1-x}Sn_x$  as a function of both Sn content and biaxial strain is shown in Fig. 1. The colored region corresponds to the case in which the  $\Gamma$  point is lower than L point in the conduction band resulting in a direct bandgap material. The uncolored region corresponds to the case of an indirect bandgap. The black

solid lines represents the band-gap of the material. The bending of these solid lines are observed close to direct/indirect bandgap transition reflecting the different dependencies of the  $\Gamma$ -valley and L-valley on composition and strain. Similarly, the same bending phenomena are observed close to the transition from compressive to tensile strain as the uppermost valence band changes between light hole and heavy hole. The area to the left of the red dashed line corresponds to  $Ge_{1-x}Sn_x$  with a compressive stress higher than strained  $Ge_{1-x}Sn_x$  grown on relaxed Ge. In practice, this can be achieved by growing  $Ge_{1-x}Sn_x$  lattice matched to  $Si_{1-y}Ge_y$ . When fully compressively strained  $Ge_{1-x}Sn_x$  is grown on Ge (red dashed line),  $Ge_{1-x}Sn_x$  is always indirect. With sufficient partial relaxation, the  $Ge_{1-x}Sn_x$  can become a direct bandgap material if it contains sufficient Sn. As a result, the minimum Sn content necessary to make  $Ge_{1-x}Sn_x$  a direct bandgap material decreases with decreasing compressive strain. This decrease in minimum Sn content continues for tensile strained. This can for example be obtained by growing strained  $Ge_{1-x}Sn_x$  on fully relaxed  $Ge_{1-y}Sn_y$  with  $x < y$ . A direct bandgap material is also obtained for tensile strained Ge (purple dashed line) with sufficiently strain which we calculated to be at least 1.8%.

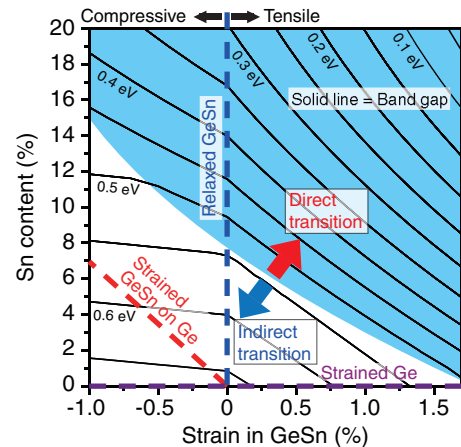


**Figure 1.** Theoretically calculated bandgap of  $Ge_{1-x}Sn_x$  as functions of Sn content and strain. The conditions to obtain direct bandgap material are fulfilled for the colored region. The calculated bandgap values are also shown. The blue and red dashed lines represent the fully relaxed  $Ge_{1-x}Sn_x$  and the strained  $Ge_{1-x}Sn_x$  pseudomorphically grown on unstrained Ge, respectively. The area between the red dashed line and the blue dashed line corresponds to partial relaxed  $Ge_{1-x}Sn_x$  epitaxially grown on Ge.

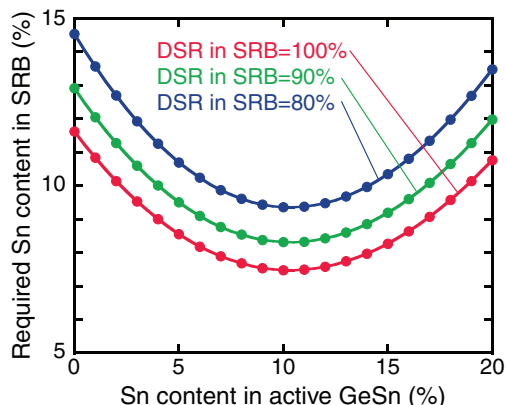


**Figure 2.** Required Sn content in an SRB to enable the deposition of a direct bandgap  $\text{Ge}_{1-x}\text{Sn}_x$  layer on top of it as a function of the Sn content in the active  $\text{Ge}_{1-x}\text{Sn}_x$  layer and for SRBs with different degrees of strain relaxation.

**Required Sn in the SRB.**—Fully strained  $\text{Ge}_{1-x}\text{Sn}_x$  on an appropriate buffer layer can suppress the introduction of additional dislocations by strain relaxation. For a given Sn content in the active  $\text{Ge}_{1-x}\text{Sn}_x$  layer, the minimum amount of strain required to obtain a direct bandgap is given by the calculation results summarized in Fig. 1. The assumption of a pseudomorphically grown active  $\text{Ge}_{1-x}\text{Sn}_x$  layer on top of the SRB allows us to estimate the required lattice constant in the SRB layer as a function of the Sn content in the active layer to realize the required strain with the constraint of  $E_{cL} = E_{cT}$  (boundary between colored and uncolored region in Fig. 1). The red curve in Fig. 2 shows the required Sn content for a fully relaxed  $\text{Ge}_{1-y}\text{Sn}_y$  SRB. In practice it is difficult to realize a fully relaxed SRB layer.<sup>11–13</sup> Therefore, we performed the same exercise for partially relaxed SRBs (Green and blue curves in Fig. 2). Independent of the DSR of the SRB, the required Sn content in the  $\text{Ge}_{1-y}\text{Sn}_y$  SRB shows a minimum for a Sn content around 10% in active  $\text{Ge}_{1-x}\text{Sn}_x$ . Because of the low Sn solubility limit, it is recommended to keep the implemented Sn content as low as possible. A fully relaxed SRB should contain at least 7.48% Sn. The required Sn concentration in the SRB increases with decreasing DSR in order to maintain the lattice constant (Fig. 2). E.g. if the SRB is only 80% relaxed we calculated the minimal required Sn concentration in the SRB to obtain a direct bandgap in the active layer to be 9.36%.

**Band offsets.**—In addition to having a direct bandgap material, carrier confinement in the gain medium is another important parameter that needs to be taken into account. The band offset between the buffer

layer and the active medium, which determines the carrier confinement under electrical or optical pumping, has to be at least 26 meV, equal to the thermal energy, for both the conduction and the valence band. As a result, for any carrier confinement, the difference between the bandgap of the SRB,  $E_{gSRB}$ , and that of the active medium,  $E_{gactive}$ , must be at least 52 meV. First, the band-offset without any electrical bias will be considered. Next, we will proceed with devices under bias where the position of the fermi-energy determined by impurity doping.

The addition of Si, which has a larger bandgap compared to Ge and Sn (Table I), into the SRB increases  $E_{gSRB}$ . This enables tuning of the band-offset between the buffer layer and the active medium. In order to maintain the  $\text{Si}_{1-y-z}\text{Ge}_y\text{Sn}_z$  SRB's lattice constant to the required value as calculated in Fig. 2, the Si content in SRB must follow the relation;

$$a_{Ge}(1 - Si\% - Sn\%) + a_{Si}Si\% + a_{Sn}Sn\% = a_{Ge}(1 - A) + a_{Sn}A$$

$$\Rightarrow Si\% = \frac{a_{Ge} - a_{Sn}}{a_{Si} - a_{Ge}}(Sn\% - A) = 3.67(Sn\% - A) \quad [4]$$

where  $Sn\%$  denotes Sn the content in the  $\text{Si}_{1-y-z}\text{Ge}_y\text{Sn}_z$  SRB, “A” denotes the required Sn content when  $\text{Ge}_{1-y}\text{Sn}_y$  is used as SRB (Fig. 2). The Sn content in the  $\text{Si}_{1-y-z}\text{Ge}_y\text{Sn}_z$  SRB has to be larger than the “A”. The “A” value is a function of Sn content in the active layer as shown in Fig. 2. Here, bowing parameters for the lattice constant are assumed not to be included in Eq. 4 as the effect in Si% is almost ignorable. According to Eq. 4, the required Si content to maintain the lattice constant of the SRB decreases with decreasing DSR as “A” increases.

The  $(E_{gSRB} - E_{gactive})/2$  values for different DSR in the SRB are calculated as function of the Sn content in the active  $\text{Ge}_{1-x}\text{Sn}_x$  layer and in the  $\text{Si}_{1-y-z}\text{Ge}_y\text{Sn}_z$  SRB, respectively (Fig. 3). If the Sn content exceeds 8%, the bandgap of the active  $\text{Ge}_{1-x}\text{Sn}_x$  layer strongly decreases with increasing Sn content as can be seen in Fig. 1. This results are reflected in Fig. 3. When the Sn content in the active region exceeds 8%, the required Si content in SRB becomes less. Eventually, a fully relaxed  $\text{Ge}_{0.92}\text{Sn}_{0.08}$  (without Si) SRB can realize 26 meV offsets if it is combined with a compressively strained  $\text{Ge}_{0.86}\text{Sn}_{0.14}$  active layer pseudomorphically grown on the SRB.

Assuming the DSR of the SRB to be 100% (Fig. 3a), pure Ge grown on  $\text{Si}_{1-y-z}\text{Ge}_y\text{Sn}_z$  SRB requires at least 14% Sn and 10% Si to obtain direct bandgap material with sufficiently high conduction and valence band offsets (>26 meV). With decreasing DSR of the SRB, a higher Sn content is required to maintain the band offsets. The window which offers confinement decreases with decreasing DSR. However, even for a DSR of the SRB as low as 80% (Fig. 3c), we expect a direct bandgap material with sufficiently high band offsets for a fully strained active  $\text{Ge}_{1-x}\text{Sn}_x$  layer with 8% Sn grown on a  $\text{Si}_{1-y-z}\text{Ge}_y\text{Sn}_z$  SRB with 12.5% Si and 13% Sn.

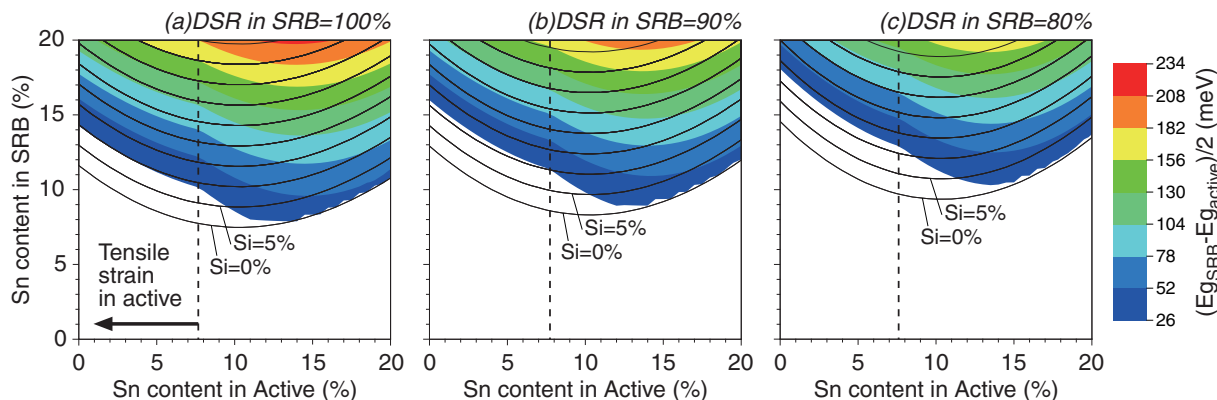


**Figure 3.** Theoretically calculated energy bandgap difference between the fully strained  $\text{Ge}_{1-x}\text{Sn}_x$  active layer epitaxially grown on a strain relaxed  $\text{Si}_{1-y-z}\text{Ge}_y\text{Sn}_z$  SRB,  $(E_{gSRB} - E_{gactive})/2$ . DSR in the SRB ranging from 80% to 100% are considered. Si contents in SRB calculated from Eq. 4 are shown as solid curves with 5% step.

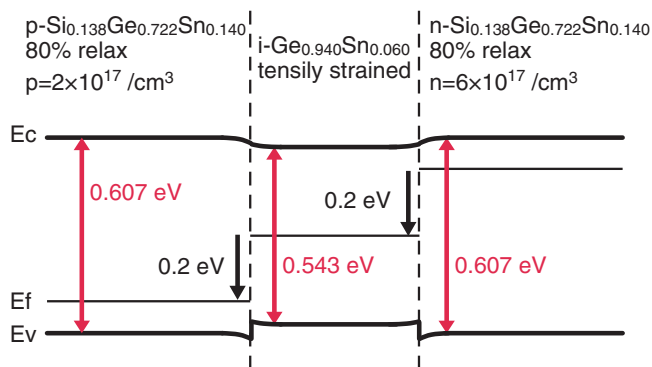


**Figure 4.** Proposed final structure for a group-IV laser consisting of fully strained direct bandgap  $\text{Ge}_{0.940}\text{Sn}_{0.060}$  embedded in 80% relaxed  $\text{Si}_{0.138}\text{Ge}_{0.722}\text{Sn}_{0.140}$  SRB layers. The drawing shows the simplified band diagram under forward bias. The valence and conduction band offsets at the hetero-interfaces are calculated from the model solid theory by comparing the energy position of valence band maxima (conduction band minima) between isolated  $\text{Ge}_{0.940}\text{Sn}_{0.060}$  and 80% relaxed  $\text{Si}_{0.138}\text{Ge}_{0.722}\text{Sn}_{0.140}$  layers.

When the active layer is under tensile strain, the laser operates at a higher differential optical gain as the light hole valence band is no longer degenerate with the heavy hole band.<sup>24</sup> In Ref. 24 it was shown that 0.25% tensile strain is sufficient to effectively increase the gain. Reducing the Sn content in the active layer from 8% to 6% (assuming 80% relaxation in the  $\text{Si}_{0.138}\text{Ge}_{0.722}\text{Sn}_{0.140}$  SRB) is expected to offer a promising structure for group-IV laser device. Compared to the strain free  $\text{Ge}_{1-x}\text{Sn}_x$  discussed above, the increase in required Sn content in the SRB is only 1%. In the given structure, the active  $\text{Ge}_{0.94}\text{Sn}_{0.06}$  layer contains 0.33% tensile strain (the critical thickness for strain relaxation is estimated to be 35~50 nm<sup>25</sup>). The calculated band gaps are 0.543 eV and 0.607 eV for the active layer and SRB, respectively. We would like to emphasize that the interface between the active layer and the SRB layer would ideally be defect-free as the active layer is coherently grown on the SRB.

Typical operation of a semiconductor laser device, typically a p-i-n diode, would be electrically pumped. As a result, the band offsets at the conduction and valence band are also required when the device is forward biased. We consider an intrinsic active  $\text{Ge}_{0.940}\text{Sn}_{0.060}$  layer pseudomorphically embedded between 80% relaxed p-type  $\text{Si}_{0.138}\text{Ge}_{0.722}\text{Sn}_{0.140}$  and n-type  $\text{Si}_{0.138}\text{Ge}_{0.722}\text{Sn}_{0.140}$  SRB. The required Fermi level shift from the mid gap equals to the applied bias for the laser operation. When 0.2 V of potential drop is observed at each interfaces, the required impurity doping needed to shift the Fermi level 0.2 eV is  $2 \times 10^{17}/\text{cm}^3$  for the top p-type  $\text{Si}_{0.138}\text{Ge}_{0.722}\text{Sn}_{0.140}$  SRB and  $6 \times 10^{17}/\text{cm}^3$  for the bottom n-type  $\text{Si}_{0.138}\text{Ge}_{0.722}\text{Sn}_{0.140}$  SRB with the final structure of p-i-n  $\text{Ge}_{1-x}\text{Sn}_x$  laser as shown in Fig. 4. The required doping concentrations have been calculated using material parameters such as intrinsic carrier concentration and effective density of state are those of pure Ge at 300 K.

### Summary

Theoretical calculations using the model solid theory were performed to design a group-IV laser stack based on a fully strained  $\text{Ge}_{1-x}\text{Sn}_x$  active layer grown on strain relaxed  $\text{Si}_{1-y-z}\text{Ge}_y\text{Sn}_z$  buffer/barrier layer. If the SRB has a sufficiently large lattice constant, the epitaxial  $\text{Ge}_{1-x}\text{Sn}_x$  layer grown on top of it will always be a direct bandgap material. The impact of the DSR on the band offset

between the active and the SRB layer has been considered. For a realistic scenario where the DSR of SRB is limited to 80%, we designed the laser device structure with a fully strained  $\text{Ge}_{1-x}\text{Sn}_x$  with 6% Sn as the active layer on top of a  $\text{Si}_{1-y-z}\text{Ge}_y\text{Sn}_z$  SRB (Si 13.8%, Sn 14%) which enables to achieve a direct bandgap  $\text{Ge}_{1-x}\text{Sn}_x$  active layer with a band offset of 26 meV to allow carrier confinement between the valence band and the conduction band. At the end, we proposed the final structure for a group-IV laser which is a fully strained  $\text{Ge}_{0.940}\text{Sn}_{0.060}$  layer embedded in  $\text{Si}_{0.138}\text{Ge}_{0.722}\text{Sn}_{0.140}$  with doping concentration of  $2 \times 10^{17}/\text{cm}^3$  for the top p-type SRB and  $6 \times 10^{17}/\text{cm}^3$  for the bottom n-type SRB assuming 0.2 V potential drop at both interfaces.

### Acknowledgment

Y. Shimura acknowledges the Research Foundation of Flanders (FWO) for granting him a fellowship within the Pegasus Marie Curie Program. We thank the financial support via the SPIRIT (Support of Public and Industrial Research using Ion Beam Technology) project (contract no. 227012) and the KU Leuven project GOA/2009/006. We also thank the imec core partners within the imec's Industrial Affiliation Program on Logic and OIO.

### References

1. D. A. B. Miller, *Proceedings of the IEEE*, **97**, 1166 (2009).
2. S. A. Srinivasan, M. Pantouvakis, S. Gupta, H. T. Chen, P. Verheyen, G. Lepage, G. Roelkens, K. Saraswat, D. Van Thourhout, P. Absil, and J. Van Campenhout, *J. Lightwave Technol.*, **34**, 419 (2016).
3. J. Liu, R. C-Aguilera, J. T. Bessette, X. Sun, X. Wang, Y. Cai, L. C. Kimerling, and J. Michel, *Thin Solid Films*, **520**, 3354 (2012).
4. D. W. Jenkins and J. D. Dow, *Phys. Rev. B*, **36**, 7994 (1987).
5. M. V. Fischetti and S. E. Laux, *J. Appl. Phys.*, **80**, 2234 (1996).
6. S. Wirths, R. Geiger, N. von den Driesch, G. Mussler, T. Stoica, S. Mantl, Z. Ikonik, M. Luysberg, S. Shiussi, J. M. Hartmann, H. Sigg, J. Faist, D. Buca, and D. Grützmacher, *Nature Photon.*, **9**, 88 (2015).
7. M. R. Bauer, J. Tolle, C. Bungay, A. V. G. Chizmeshya, D. J. Smith, J. Menéndez, and J. Kouvetakis, *Solid State Commun.*, **127**, 355 (2003).
8. Y.-Y. Fang, J. Xie, J. Tolle, R. Roucka, V. R. D'Costa, A. V. G. Chizmeshya, J. Menéndez, and J. Kouvetakis, *J. Am. Chem. Soc.*, **130**, 16095 (2008).
9. J. Menéndez and J. Kouvetakis, *Appl. Phys. Lett.*, **85**, 1175 (2004).
10. G. Chang, S.-W. Chang, and S. L. Chuang, *IEEE J. Quantum Electron.*, **46**, 1813 (2010).
11. Y. Shimura, N. Tsutsui, O. Nakatsuka, A. Sakai, and S. Zaima, *Thin Solid Films*, **518**, S2 (2010).
12. F. Gencarelli, B. Vincent, J. Demeulemeester, A. Vantomme, A. Moussa, A. Franquet, A. Kumar, H. Bender, J. Meersschaet, W. Vandervorst, R. Loo, M. Caymax, K. Temst, and M. Heyns, *ECS J. Solid State Science and Technology*, **2**, P134 (2013).
13. S. Wirths, Z. Ikonik, N. von den Driesch, G. Mussler, U. Breuer, A. T. Tiedemann, P. Bernardy, B. Holländer, T. Stoica, J. M. Hartmann, D. Grützmacher, S. Mantl, and D. Buca, *ECS Trans.*, **64**, 689 (2014).
14. F. A. Trumbore, *J. Electrochem. Soc.*, **103**, 597 (1956).
15. C. G. Van de Walle, *Phys. Rev. B*, **39**, 1871 (1989).
16. D. De Salvador, M. Petrovich, M. Berti, F. Romanato, E. Napolitani, A. Drigo, J. Stangl, S. Zerlauth, M. Mühlberger, F. Schäffler, G. Bauer, and P. C. Kelires, *Phys. Rev. B*, **61**, 13005 (2000).
17. Y.-H. Li, A. Walsh, S. Chen, W.-J. Yin, J.-H. Yang, J. Li, J. L. F. Da Silva, X. G. Gong, and S.-H. Wei, *Appl. Phys. Lett.*, **94**, 212109 (2009).
18. V. R. D'Costa, Y.-Y. Fang, J. Tolle, J. Kouvetakis, and J. Menéndez, *Thin Solid Films*, **518**, 2531 (2010).
19. U. Schmid, N. E. Christensen, and M. Cardona, *Solid State Commun.*, **75**, 39 (1990).
20. C. N. Ahmad and A. R. Adams, *Phys. Rev. B*, **34**, 2319 (1986).
21. T. Brudevoll, D. S. Citrin, M. Cardona, and N. E. Christensen, *Phys. Rev. B*, **48**, 8629 (1993).
22. J. Liu, D. D. Cannon, K. Wada, Y. Ishikawa, D. T. Danielson, S. Jongthammanurak, J. Michel, and L. C. Kimerling, *Phys. Rev. B*, **70**, 155309 (2004).
23. J. D. Gallagher, C. L. Senaratne, J. Kouvetakis, and J. Menéndez, *Appl. Phys. Lett.*, **105**, 142102 (2014).
24. J. Liu, X. Sun, D. Pan, X. Wang, L. C. Kimerling, T. L. Koch, and J. Michel, *Optics Express*, **15**, 11272 (2007).
25. J. W. Matthews and A. E. Blakeslee, *J. Cryst. Growth*, **27**, 118 (1974).